Pseudomonas putida biofilm dynamics following a single pulse of silver nanoparticles

1 **Accepted publication pre-print version**

2 ***Pseudomonas putida* biofilm dynamics following a single pulse of silver nanoparticles**

3 Florian Mallevre, Teresa F. Fernandes, Thomas J. Aspray*

4 School of Life Sciences, NanoSafety Research Group, Heriot-Watt University, Edinburgh

5 EH14 4AS, Scotland, UK

6 * Corresponding author. Tel.: +44 (0)131 451 3974; fax: +44 (0)131 451 3009; e-mail address:

7 T.J.Aspray@hw.ac.uk, thomasaspray@gmail.com (T. J. Aspray).

Graphical abstract

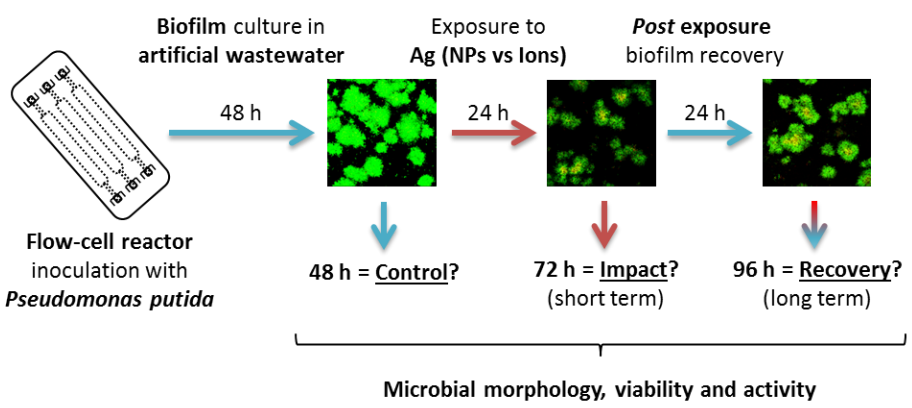

Abstract

Pseudomonas putida mono-species biofilms were exposed to silver nanoparticles (Ag NPs) in artificial wastewater (AW) under hydrodynamic conditions. Specifically, 48 h old biofilms received a single pulse of Ag NPs at 0, 0.01, 0.1, 1, 10 and 100 mg L^{-1} for 24 h in confocal laser scanning microscopy (CLSM) compatible flow-cells. The biofilm dynamics (in terms of morphology, viability and activity) were characterised at 48, 72 and 96 h. Consistent patterns were found across flow-cells and experiments at 48 h. Dose dependent impacts of NPs were then shown at 72 h on biofilm morphology (*e.g*. biomass, surface area and roughness) from 0.01 mg L^{-1}. The microbial viability was not altered below 10 mg L^{-1} Ag NPs. The activity (based on the D-glucose utilisation) was impacted by concentrations of Ag NPs equal and superior to 10 mg L^{-1}. Partial recovery of morphology, viability and activity were finally observed at 96 h. Comparatively, exposure to Ag salts resulted in *ca*. one order of magnitude higher toxicity when compared to Ag NPs. Consequently, the use of a continuous culture system and incorporation of a recovery stage extends the value of biofilm assays beyond the standard acute toxicity assessment.

Keywords

Biofilm; Flow-Cell Reactor; *Pseudomonas putida*; Silver Nanoparticle; Recovery; Ecotoxicology.

1. Introduction

Current interest in engineered nanoparticles (NPs) is clear given their various attractive physico-chemical properties (Ju-Nam and Lead 2008; Rai *et al*., 2014). There are nevertheless legitimate concerns regarding the actual risk associated with the emergence of anthropogenic NPs in the environment (Duester *et al*., 2014; Eduok *et al*., 2013). Reported environmental concentrations of the majority of NPs in freshwater systems are in the $\mu g\ L^{-1}$ range and likely to increase due to the wide applications of NPs in societal and medical products (Gottschalk *et al*., 2013; Ju-Nam and Lead 2008; Rai *et al*., 2014). Consequently, the potential adverse effects of NPs on microorganisms in environmental systems (natural and otherwise) need to be appraised.

Bacteria have already been used intensively in nano(eco)toxicology, especially using planktonic cultures (Holden *et al*., 2014; Kahru and Ivask, 2013). Biofilms, defined as self-produced matrix enclosed mono or multi-species microbial communities that adhere to biological or non-biological surfaces or interfaces (Stewart and Franklin, 2008), are nonetheless referred as the main living form of bacteria in the environment (Hall-Stoodley *et al*., 2004). Structurally organized, dynamic and complex ubiquitous biological systems, biofilms have in addition essential beneficial implications (*e.g*. facilitators within the natural environment or in the treatment of wastewaters) (Hall-Stoodley *et al*., 2004; Stewart and Franklin, 2008). Consequently, biofilm based assays represent a desirable source of information in nano(eco)toxicology.

Despite their relevance, only a handful of nano(eco)toxicological studies has been carried out using biofilms to date. Assays performed under static conditions (*i.e*. here referred to as static biofilms) using microtitre plates or glass slides, coupled with spectrophotometry or confocal laser scanning microscopy (CLSM), have been reported (Choi *et al*., 2010; Dong and Yang, 2014; Dror Ehre *et al*., 2010; Inbakandan *et al*., 2013; Martinez-Gutierrez *et al*., 2013; Radzig *et al*., 2013; Raftery *et al*., 2014). However, biofilms obtained under hydrodynamic conditions (*i.e*. here referred to as non-static biofilms) are fully hydrated, planktonic free and mature structures compared to the static biofilms (Buckingham-Meyer *et al*., 2007; Crusz *et al*., 2012; Weiss Nielsen *et al*., 2011). Studies based on non-static biofilms are therefore gradually emerging using diverse rotating biological contactor and reactors

(Fabrega *et al*., 2009; Hou *et al*., 2014; Martinez-Gutierrez *et al*., 2013; Park *et al*., 2013). Unlike most reactors, the flow-cell systems present the additional advantages of real time, non-invasive and non-destructive versatile studies (Crusz *et al*., 2012; Weiss Nielsen *et al*., 2011). Consequently, a high potential of assay development is associated with the use of flow-cell reactors.

Applications of flow-cell reactors were reported in (eco)toxicology for the testing of silver sulfadiazine and solvent styrene on *Pseudomonas* spp. biofilms (Bjarnsholt *et al*., 2007; Halan *et al*., 2011). Examples in nano(eco)toxicology are particularly scarce at the present time as the sole contribution is the study by Fabrega *et al*. (2009) where the interactions between Ag NPs and *Pseudomonas putida* biofilms were investigated (*e.g*. accumulation and uptake of NPs). These authors especially stressed the need of complementary studies dedicated to the assessment of long term effects (*i.e*. including recovery) of NPs to complex materials such as biofilms. This was further emphasised in recent literature (Handy *et al*., 2012) as an area not being considered in most of the nano(eco)toxicological studies published so far.

The present study builds on these pioneer examples (Bjarnsholt *et al*., 2007; Fabrega *et al*., 2009; Halan *et al*., 2011) and aims to assess the temporal impact following a single pulse of NPs on non-static mono-species biofilm morphology, viability and activity using flow-cell reactors. Silver (Ag) is prioritised given that it is a well-known bactericidal agent and one of the most widely used NPs in a large range of applications (Morones *et al*., 2005; Rai *et al*., 2014). *P. putida* based biofilms are considered since they are used with flow-cell reactors and are commonly proposed as an environmental bacterial model (Bjarnsholt *et al*., 2007; Fabrega *et al*., 2009; Halan *et al*., 2011). Consequently, the dynamics (considering the impact in the short term as well as the potential recovery in the long term) of mature *P. putida* biofilms (considering morphology, viability and activity) in response to a single pulse of Ag NPs and salts are here reported and discussed.

2. Material and methods

2.1. Material

The biofilm reactor consisted of inverted Perspex flow-cells (CLSM compatible) and bubble traps purchased from DTU Systems Biology (Lyngby, Denmark) used in combination with 24 x 50 mm glass coverslips (1.5 mm thick) from SLS UK Ltd and silicone (Versilic) and Marprene (Watson Marlow UK Ltd) tubings as reported previously (Crusz *et al*., 2012; Weiss Nielsen *et al*., 2011). Representative Ag NPs (*i.e*. JRCNM03000a also named Ag NM-300K NPs, which are negatively charged nanoparticles with a primary size *ca*. 15 nm delivered in suspension at 10 % (w/v) in 4 % (v/v) each of polyoxyethylene glycerol trioleate and polyoxyethylene (20) sorbitan mono-laurat) were obtained from the European Commission's Joint Research Centre (Ispra, Italy) and characterised previously (Klein *et al*., 2011; Mallevre *et al*., 2014). The Filmtracer Live/Dead® Biofilm Viability Kit was purchased from Life Technologies UK Ltd. D-glucose, silver nitrate ($AgNO_3$), phenol and sulphuric acid were from Fisher Scientific UK Ltd. Rely^{+}On Virkon® disinfectant was from DuPont. A silver single element standard was purchased from Perkin Elmer UK Inc.

2.2. Methods

2.2.1. Culture of *P. putida* mono-species biofilms in a flow-cell reactor

Biofilms were cultured under hydrodynamic (laminar) conditions using parallelised flow-cells as schematised in Figure 1. Wastewater isolated *Pseudomonas putida* BS566*::luxCDABE* (hereafter referred to as *P. putida BS566*) (Wiles *et al*., 2003) was used as a model bacterium for establishing mono-species biofilms. All experiments were performed in artificial wastewater (AW), the composition of which is reported elsewhere (Mallevre *et al*., 2014) using D-glucose at 0.5 % (w/v) as sole carbon source.

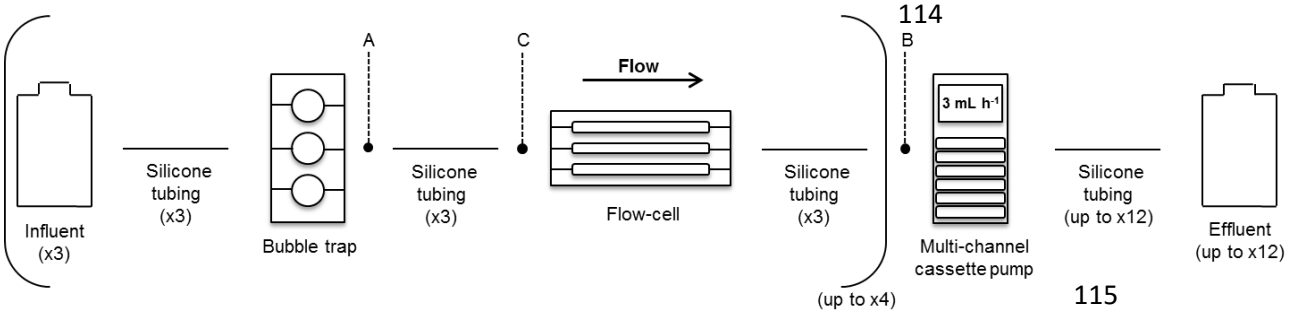

Fig. 1: Schematic diagram of the set up reactor. The reactor comprised parallelised CLSM compatible flow-cells (bearing independent channels) complying with the above presented

configuration. A, B and C refer to key actions performed during the inoculation process: clamp off in A, dis-connect in B then inoculate in C.

The set up reactor was cleaned with Virkon® 1 % (w/v) then extensively washed with sterile deionised water at 15 mL channel^{-1} h^{-1} using a 205U multi-channel cassette pump (Watson Marlow UK Ltd). The channels were then filled with sterile AW and left at minimal flow rate overnight. Prior to the inoculation, the bacterium was pre-cultured overnight at 28 ± 2 °C under shaking conditions (140 rpm) in AW then diluted in order to reach a final concentration *ca*. 10^7 CFU mL^{-1} (corresponding to a dilution about 1:100e). Each channel was then independently inoculated with 200 µL of freshly prepared cell suspension by: clamping off the tubing upstream of each flow-cell (Fig. 1, position A), disconnecting the tubing downstream of the flow-cells (Fig. 1, position B) and injecting the bacterial suspension within the channels (Fig. 1, position C). After inoculation, the tubings were re-connected and dis-clamped; the flow-cells were then incubated 1 h (*i.e*. flow off, glass coverslip on bottom). The biofilms were cultured (*i.e*. glass coverslip on top) for 48 h in AW with a consistent flow rate of 3 mL channel^{-1} h^{-1}.

2.2.2. Experimental scenario of culture, exposure and recovery

Stock suspensions of Ag NPs at 100 mg L^{-1} were freshly prepared in AW prior to each experiment, sonicated (2 x 8 min in a Kerry ultrasonic water bath at 38 ± 10 KHz), then serially diluted to give final concentrations of 0, 0.01, 0.1, 1, 10 and 100 mg L^{-1} applied for 24 h at 3 mL channel^{-1} h^{-1} on 48 h old biofilms. Ag ions (applied as $AgNO_3$) were similarly tested at final concentrations of 0, 0.001, 0.01, 0.1, 1 and 10 mg L^{-1}. Virkon® 1 % (w/v) was tested as a toxicant positive control. After exposure, upstream tubings were purged and the system filled with fresh AW (*i.e.* free from any toxicant) for an additional 24 h of culture at 3 mL channel^{-1} h^{-1}. Three time points were defined: 48 h (*i.e*. assessing the biofilm establishment and culture), 72 h (*i.e.* assessing the short term effects of the exposure) and 96 h (*i.e.* assessing the long term effects of the exposure and the potential recovery of the biofilms).

2.2.3. Biofilm morphology, viability and activity characterisation

Morphology and viability of the biofilms were characterised within the flow-cells at 48, 72 and 96 h by CLSM in a non-destructive manner. Image capture was performed on a Leica

Microsystems TCS SP2 inverted CLSM with a HCX APO CS 63x 1.4 oil immersion lens after staining with the Filmtracer Live/Dead® Biofilm Viability Kit following recommendations of the manufacturer. Both Syto® 9 (green, characterising the live cells) and Propidium Iodide (PI, red, characterising the dead cells) stains were excited with a laser source at 488 nm in a unidirectional mode at speed of 400 Hz. Emissions were simultaneously monitored *via* distinct photomultipliers set at 510 - 530 nm and 610 - 630 nm, respectively. A total of seven z-stacks (characterised by 100 images at 512 x 512 in resolution in a consistent 100 µm thickness window) were randomly registered *per* condition (*i.e*. *per* channel) for each time point in all experiments. CLSM images were processed by the Leica Microsystems LAS AF Lite software for viability and analysed with the COMSTAT 1 program (Danish Technical University) using Matlab R2013b (MathWorks, USA) software for morphology (*e.g*. total biomass, maximum thickness, mean thickness, roughness coefficient and surface area) as described in Heydorn *et al*. (2000). Data from the COMSTAT based analysis were further processed following:

Relative evolution (in % terms) = (results at y - results at x) / (results at x) *eq. 1*

where x, y are 48 and 72 h or 72 and 96 h, respectively.

The microbial activity was assessed by the monitoring of the D-glucose utilisation (*i.e*. sole carbon source) within the experimental scenario. The amount of D-glucose was quantified in both influent and effluent collected samples at 48, 72 and 96 h (after filtration at 0.2 µm) following the phenol-sulphuric acid assay based protocol described elsewhere (Fournier, 2001). Then the percentage of D-glucose remaining in effluents (hereafter referred to as D-glucose ratio) was calculated for each condition and time point.

2.2.4. Nanoparticle characterisation

The Ag NPs were analysed by UV-Visible spectrophotometry (UV-Vis) using an Evolution 600 spectrophotometer (Fisher Scientific, UK) and by Dynamic Light Scattering (DLS) using a Nanosizer (Malvern, UK) as described in Mallevre *et al*. (2014) in influent and effluent collected samples at 48, 72 and 96 h (after filtration at 0.2 µm). The concentration of total silver element was measured in collected samples by Atomic Absorption Spectroscopy (AAS) using an AAnalyst 200 Spectrometer (Perkin Elmer, UK) calibrated with an Ag single element

standard at concentrations of 0.156, 0.312, 0.625, 1.25, 2.5 and 5 mg L^{-1} (R^2 = 0.9986 ± 0.0004, n = 4). The size distribution (z-average) and zeta potential data were treated with the Zetasizer software (Malvern, UK).

3. Results

3.1. Characterisation of the *P. putida* control biofilms at 48 h

Representative examples of CLSM z-stack obtained *ante* exposure are presented in Figure 2 (top row). *P. putida* BS566 formed distinct and consistent microcolonies in D-glucose supplemented AW across channels. This was confirmed across experiments as well *via* the morphology related information obtained by the COMSTAT based analysis. Specifically (considering 210 z-stacks in total with n = 5), control biofilms at 48 h were consistently characterised by comparable biomass, maximum and mean thickness, roughness and surface area of: 27.5 ± 2.6 μm^3 μm^{-2}, 94.4 ± 3 µm, 50.2 ± 2.8 µm, 0.48 ± 0.01 and 3.2 ± 0.1 10^6 μm^2, respectively. No red staining (*i.e*. dead cells) was observed. From a microbial activity standpoint (Fig. 3), *ca*. 70 % of the original D-glucose loading was consistently found in the effluents across channels and experiments.

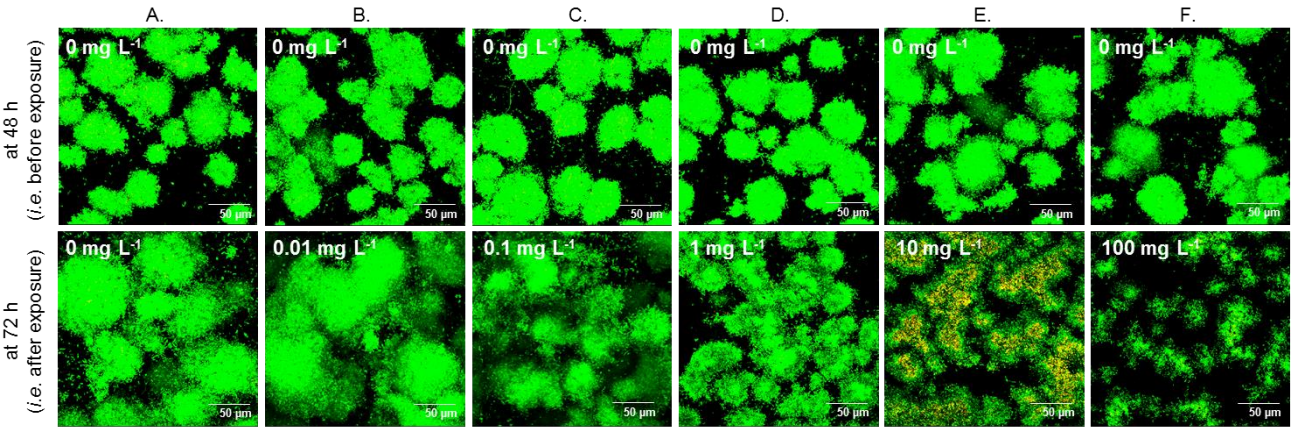

Fig. 2: Qualitative characterisation of the biofilm morphology *ante* and *post* exposure to Ag NPs. *P. putida* biofilms were cultured for 48 h then exposed to 0, 0.01, 0.1, 1, 10 and 100 mg L^{-1} Ag NPs for 24 h (from A to F, respectively). Biofilms were analysed by CLSM after live/dead staining at 48 h (*i.e*. *ante* exposure, top row) and at 72 h (*i.e*. *post* exposure, bottom row). Representative examples of maximised z-stack are shown. Each image represents 1 out of 7 z-stacks randomly registered *per*

condition for 1 experiment. Additional examples of result at 72 h from the replicate experiments (n = 5) are presented in the supplementary material (Fig. S1). Scale is 50 µm wide.

3.2. Characterisation of the *P. putida* exposed biofilms at 72 h

Representative examples of CLSM z-stack registered at 72 h *post* exposure to a single pulse of 0, 0.01, 0.1, 1, 10 and 100 mg L^{-1} Ag NPs for 24 h are presented in Figure 2 (bottom row). Additional examples are provided in the supplementary material (Fig. S1).

From a morphological viewpoint, larger and less discrete microcolonies were observed at 72 h than at 48 h for the control (Fig. 2, column A). Biofilms exposed to 0.01 mg L^{-1} Ag NPs showed comparable development overall (Fig. 2, column B). However the biofilm development was visibly altered at 0.1 mg L^{-1}; dose dependent impacts of Ag NPs were then observed with, finally, sparsely distributed residues of microcolonies characterised at 100 mg L^{-1} (Fig. 2, columns C - E). Red staining was obtained (in 3 out of 5 experiments) at 10 mg L^{-1} exclusively.

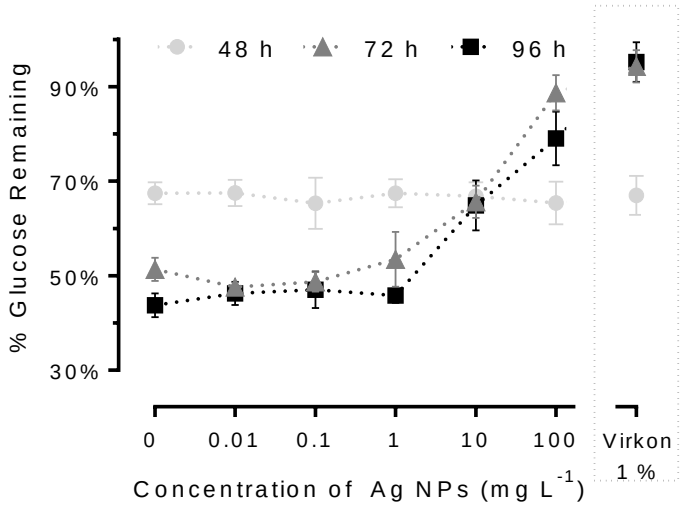

Fig. 3: Quantitative characterisation of the microbial activity (Ag NP case). Samples collected upstream (*i.e*. in influents) and downstream (*i.e*. in effluents) of the flow-cells at 48, 72 and 96 h were used for D-glucose quantification *via* the phenol - sulphuric acid assay. Presented data are mean ± SEM (n = 4) of the calculated D-glucose remaining (in % terms) in effluents *per* tested condition. Corresponding results for the Ag ion case are shown in Figure S3. The detailed findings

from the statistical analysis *via* multiple t-tests (corrected with the Holm-Sidak method) considering two parameters at a time are shown in the supplementary material (Fig. S4).

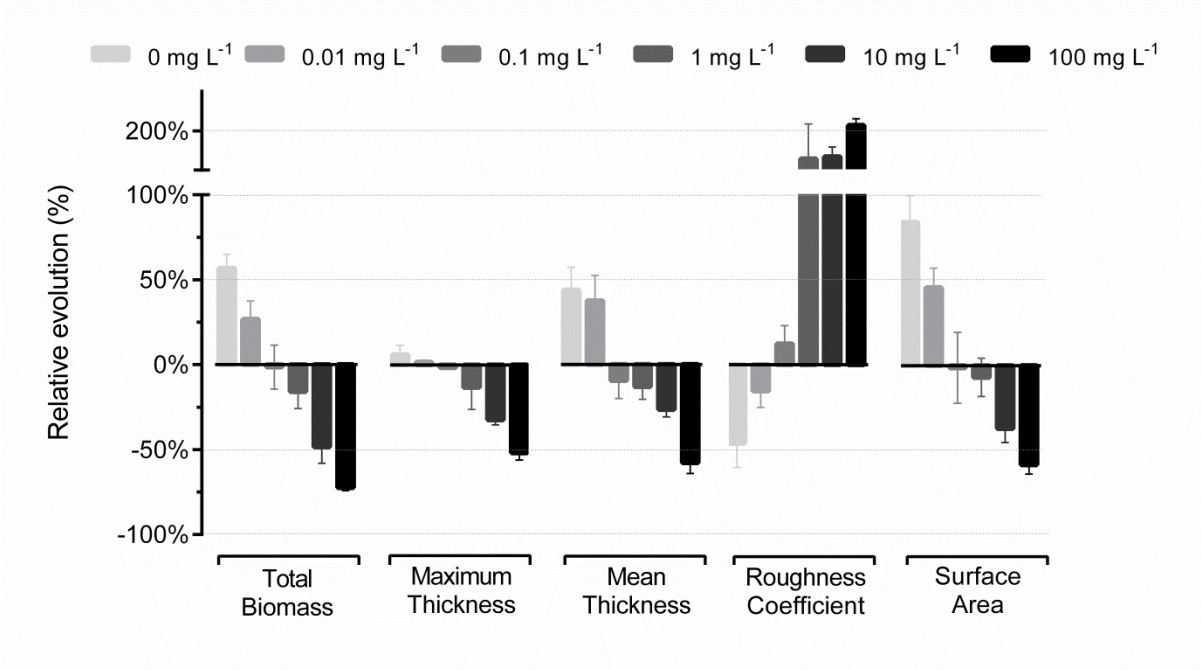

Fig. 4: Quantitative characterisation of the biofilm morphology *post* exposure to Ag NPs. Histogram of the relative evolution (in % terms) of the descriptive biofilms parameters (*e.g*. total biomass, maximum thickness, mean thickness, roughness and surface area) *post* exposure for 24 h to Ag NPs at 0, 0.01, 0.1, 1, 10 and 100 mg L^{-1} is presented. Data, calculated *per* channel as (results at 72 h - results at 48 h) / (results at 48 h) after the COMSTAT analysis of the registered z-stacks, are mean ± SEM (n = 5). For each experiment 7 z-stacks were analysed *per* channel (*i.e*. *per* condition) at both time points.

The corresponding information from the COMSTAT analysis is shown in Figure 4. Overall results confirmed the dose dependent impact of Ag NPs on biofilm morphology following a 24 h pulse. The trend was characterised by a decrease in total biomass, thickness, surface area and an increase in roughness with increasing concentrations of NPs. More specifically, non-exposed biofilms gained 57 ± 8 % of biomass in 24 h; meanwhile the 0.01 mg L^{-1} exposed biofilms gained significantly less (27 ± 11 %) (as determined *via* multiple t-tests using the Holm-Sidak method, reporting significance with p value < 0.05). The altered evolution of both the roughness and surface area related information was correlatively

observed at 0.01 mg L^{-1} compared to the non-exposed biofilms. Impact on thickness was not evident at 0.01 mg L^{-1} though. Comparatively at 0.1 mg L^{-1} Ag NPs, evident impacts on biomass, roughness, surface area and mean thickness were observed compared to the control; according to the COMSTAT results *post* exposure biofilms were *in fine* rather similar to biofilms characterised *ante* exposure. The next concentrations of 1, 10 and 100 mg L^{-1} led to consistent dose dependent results with detrimental effects at 100 mg L^{-1} resulting in *ca*. 75 % of the biomass and *ca*. 50 % of the thickness and surface area being lost when compared to the respective biofilm characteristics before exposure. Similarly, the roughness was increased by more than 200 % whereas non-exposed biofilms had there roughness decreased by *ca*. 50 % for the same 24 h period.

Regarding the microbial activity, comparable amounts of D-glucose (*ca*. 50 % of the original loading) were found in effluents at 72 h *post* exposure to 0, 0.01 and 0.1 mg L^{-1} Ag NPs (Fig. 3). Results were found significantly different (*i.e*. lower D- glucose ratios, increased activity) compared to results at 48 h. Percentages of remaining D-glucose between 90 % and 100 % were obtained *post* exposure to 100 mg L^{-1} Ag NPs and Virkon® 1 %; results which were found significantly different from data at 48 h with the same channels and from data at 72 h with the other channels. Results obtained *post* exposure to 10 mg L^{-1} (*ca*. 70 % of the original loading) were non-significantly different to those obtained at 48 h. The intermediate concentration of 1 mg L^{-1} showed the largest SEM of the 72 h data with D-glucose ratios varying between 45 % and 60 %; results which were found significantly different from data at 48 h but not from 0.1 mg L^{-1} and 10 mg L^{-1} related data at 72 h.

Parallel experiments were performed with Ag ions at 0, 0.001, 0.01, 0.1, 1 and 10 mg L^{-1} (n = 3). Comparable dose dependent toxicity patterns were observed overall on morphology (Fig. S2, top row) and activity (Fig. S3) but shifted by at least one order of magnitude, the Ag ions being more toxic than the tested Ag NPs. Red staining (*i.e*. dead cells) occurred consistently after exposure to 1 and 10 mg L^{-1}. No biofilms were visible at 72 h after exposure to Virkon® 1 % (data not shown) as a positive control. Exposure to Ag NM-300K NP dispersant only has already been shown not to be toxic *per se* to *P. putida* elsewhere (Mallevre *et al*., 2014).

3.3. Characterisation of the *P. putida* recovering biofilms at 96 h

Biofilms were left to recover for 24 h in AW *post* exposure. Examples of characteristic CLSM z-stack registered at 96 h for selected conditions (0, 0.01, 1 and 100 mg L^{-1}) along with the relative evolution (in % terms) of selected descriptive parameters (total biomass and mean thickness) are presented in Figure 5. Additional examples of CLSM result from replicate experiments are proposed in the supplementary material (Fig. S4).

From a morphological viewpoint (Fig. 5 A), the non-exposed biofilms were found to have developed, gaining more than 15 % in biomass and 6 % in mean thickness compared to results at 72 h. Comparatively, the exposed biofilms showed various patterns at 96 h as they were clearly recovering at 0.01 mg L^{-1} (+23 ± 8 % in biomass and +35 ± 12 % in mean thickness, no dual staining; Fig. 5 B) and struggling for survival at 100 mg L^{-1} (+7 ± 4 % in biomass and -2 ± 21 % in mean thickness, dual staining; Fig. 5 D). Very variable results across experiments were obtained at 1 mg L^{-1} with evolutions in biomass and mean thickness up to +50 % and +20 % or down to -10 % and 0 %, respectively (Fig. 5 C). Dual staining as well as possibly re-structuring microcolonies (*i.e*. presence of filaments) were also reported at 1 mg L^{-1}. Tested 0.1 and 10 mg L^{-1} concentrations led to similar dose dependent results (Fig. S5).

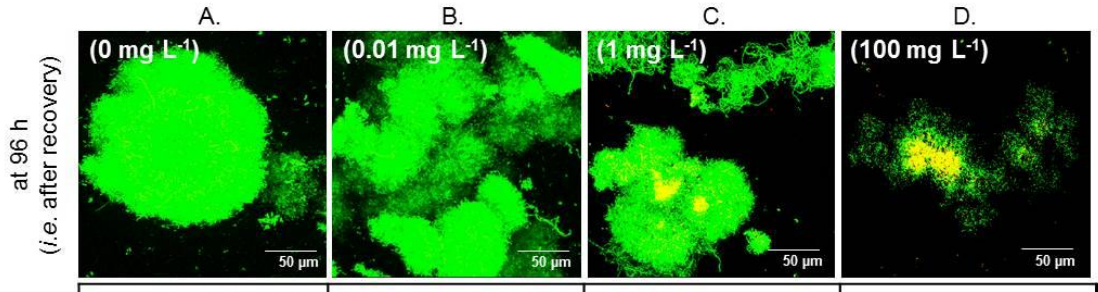

+ 17 ± 1 %	+ 23 ± 8 %	+ 23 ± 30 %	+ 7 ± 4 %	Total Biomass ($\mu m^3\ \mu m^{-2}$)
+ 6 ± 4 %	+ 35 ± 12 %	+ 10 ± 10 %	- 2 ± 21 %	Mean Thickness (µm)

Fig. 5: Biofilm morphology recovery assessment. Representative examples of maximised z-stack registered at 96 h following the recovery period after exposure to 0 (A), 0.01 (B), 1 (C) and 100 mg L^{-1} (D) Ag NPs are shown. Each image represents 1 out of 7 z-stacks registered *per* condition for 1 experiment. Results following other tested concentrations of Ag NPs (0.1 and 10 mg L^{-1}) as well as additional examples of result for replicate experiments (n = 3) are presented in the supplementary material (Fig. S5). Scale is 50 µm wide. The corresponding relative evolution (in % terms, according to *eq. 1*) in total biomass and mean thickness calculated between 72 and 96 h is also presented.

Regarding the microbial activity (Fig. 3), comparable D-glucose ratios close to 45 % were observed at 96 h from 0 mg L^{-1} to 1 mg L^{-1} tested NP concentrations. Significantly higher ratios *ca.* 70 % and 80 % (*i.e*. decreased microbial activity) were obtained for 10 and 100 mg L^{-1} Ag NPs. Overall results at 96 h were not found significantly different compared to percentages of D-glucose remaining calculated at 72 h (Fig. S4) but they were found significantly different (up to 1 mg L^{-1}) compared to results obtained at 48 h.

Experiments with Ag ions at 0, 0.001, 0.01, 0.1, 1 and 10 mg L^{-1} led to more efficient recovery patterns (n = 3) (Fig. S2, bottom row; Fig. S3; Fig. S4). Overall results at 96 h were found significantly different (up to 1 mg L^{-1}) from the ratios calculated at 72 h (Fig. S4). No biofilms were visible at 96 h *post* exposure to Virkon® 1 % (data not shown); percentages of D-glucose remaining in effluents were found consistently *ca*. 95 % of the original loading (Fig. 3).

3.4. Characterisation of Ag NPs within the experimental scenario

Ag NPs were characterised by DLS and UV-Vis after sampling upstream (*i.e*. in influents) and downstream (*i.e*. in effluents) of the flow-cells at 48, 72 and 96 h. As shown in Figure 6 A, UV-Vis spectra of Ag NPs, characterised by a sole peak *ca.* 413 nm (0.9 a.u.), were comparable at the beginning and at the end of the 24 h exposure period upstream of the flow-cells. In downstream samples: no peak was observed at 48 h, non-comparable profiles characterised by a sole peak *ca*. 415 nm (0.4 a.u.) were then obtained at 72 h. No specific peak was registered at 96 h regardless of the sample. As shown in Figure 6 B, comparable hydrodynamic size and zeta potential data were obtained by DLS at both 48 and 72 h in upstream samples: 51 ± 1.4 nm and -4.8 ± 0.8 mV, 46.7 ± 2.8 nm and -3.1 ± 1 mV, respectively. In downstream samples, hydrodynamic size and zeta potential results of 155.2 ± 14.6 nm and -12.9 ± 0.5 mV were respectively obtained at 72 h; 48 h samples were not suitable for DLS analysis (*i.e*. due to the absence of NPs). Results at 72 h were found significantly different between both types of sample. Mean polydispersity index (PDI) was 0.46 ± 0.02. Samples from 96 h were not suitable for DLS analyses either (data not shown).

Ag concentrations (*i.e*. 1, 10 and 100 mg L^{-1}) were confirmed by AAS in upstream samples at both 48 and 72 h. Comparatively, the respective concentrations in downstream samples

returned to be 69 ± 5 %, 51 ± 10 % and 89 ± 7 % of the concentrations measured in upstream samples when tested at 72 h. The concentration of Ag was below the lower detection limit of the apparatus (*i.e.* < 0.1 mg L^{-1}) when tested at 96 h regardless of the sample.

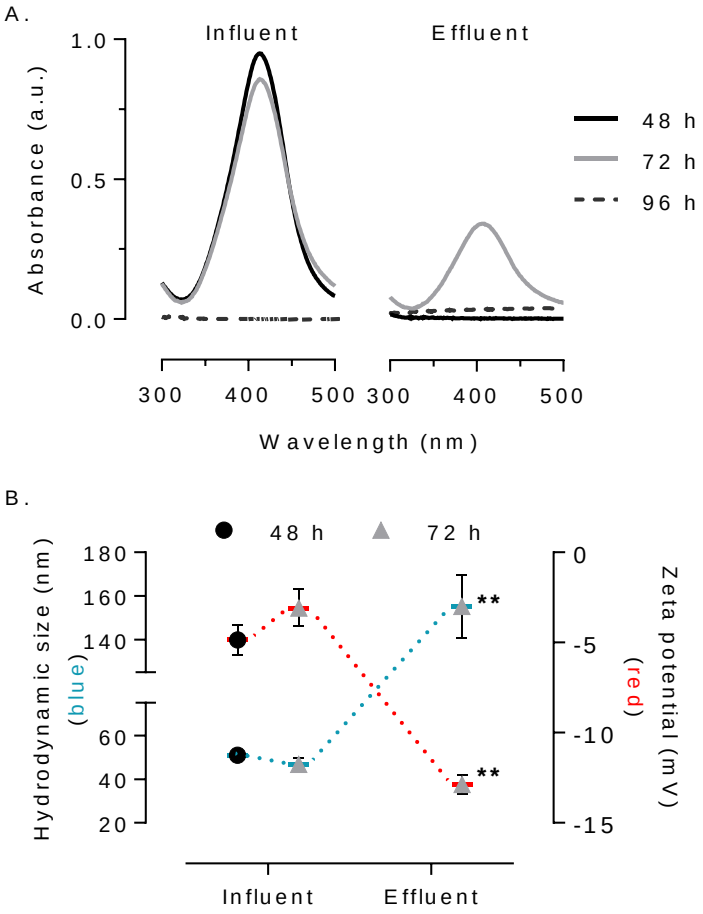

Fig. 6: Ag NP characterisation. Samples were collected upstream (*i.e.* in influents) and downstream (*i.e.* in effluents) of the flow-cells at 48, 72 and 96 h then characterised by DLS (A) and UV-Vis (B) when applicable. Data are mean ± SEM (n = 3) when tested at 10 mg L^{-1}. Significantly different between samples *via* multiple t-tests corrected with Holm-Sidak with a *p* value < 0.05 (**).

4. Discussion

4.1. Short term effects

We have shown previously (Mallevre *et al*., 2014) that the tested NPs (*i.e*. Ag NM-300K representative NPs from the OECD) were toxic to planktonic *P. putida* in AW with IC_{50} values *ca*. 5 mg L^{-1} after 1 h of exposure and that Ag ions (applied as $AgNO_3$) were comparatively at least ten times more toxic. The toxicity of Ag NPs to planktonic bacteria was mainly reported in the 1 - 10 mg L^{-1} range (Chernousova and Epple, 2013) and the frequent higher toxicity of Ag ions compared to NPs was equally reported (Notter *et al*., 2014). The toxicity of Ag NPs to various static biofilms was also reported in the literature (Choi *et al*., 2010; Dror Ehre *et al*., 2010; Inbakandan *et al*., 2013; Martinez-Gutierrez *et al*., 2013; Radzig *et al*., 2013; Raftery *et al*., 2014). Overall conclusions emphasised that Ag NPs were harmless below 1 mg L^{-1}, inhibitory in the 1 - 10 mg L^{-1} range and lethal above 100 mg L^{-1}. The higher resistance of biofilms, under hydrodynamic conditions, compared to the planktonic cells supports previous findings using static biofilms (Choi *et al*., 2010; Inbakandan *et al*., 2013; Martinez-Gutierrez *et al*., 2013; Radzig *et al*., 2013; Raftery *et al*., 2014).

From a non-static biofilm viewpoint, there are too few studies using flow-cell reactors at the present time to draw conclusive trends. Pioneer works of Bjarnsholt *et al*. (2007) showed toxic effects of Ag sulfadiazine *ca*. 10 mg L^{-1} on mature *Pseudomonas* spp. biofilms. Fabrega *et al*. (2009) thereafter discussed the accumulation of Ag NPs onto and into *Pseudomonas* spp. biofilms and reported the absence of impact on viability up to 2 mg L^{-1}. Correlatively herein, the viability of biofilms was not visibly affected *post* exposure to a single 24 h pulse of Ag NPs at 1 mg L^{-1} and below. However, the variable observation of dead cells (*i.e*. in 3 out of 5 experiments) at 10 mg L^{-1} may inform about a transient state in the biofilm response to bactericidal (*i.e*. biofilm-cidal) doses of NPs. In light of this, the absence of visible dead cells at 100 mg L^{-1} (certainly removed by the flow) is not a proof of unaltered viability but a testimony of biofilm temporal response as supported by previous studies with other chemicals (Bridier *et al*., 2011; Skogman *et al*., 2012; Tote *et al*., 2010). Despite being frequently reported, the direct comparison of the planktonic versus biofilm information may be nevertheless rather inappropriate (*i.e*. the biofilm associated cells are differentiated from the planktonic cells by reduced growth rate, up and down gene regulation, ability to show

coordinate behaviour and generation of extracellular polymeric matrix) (Booth *et al*., 2011; Bridier *et al*., 2011). Considering the "worst case scenario", disperse microcolonies were visible *post* exposure to a single 24 h pulse of 100 mg L^{-1} Ag NPs; the non-static *P. putida* biofilms were therefore more tolerant to Ag NPs than the planktonic cells (Chernousova and Epple, 2013; Mallevre *et al*., 2014). In terms of morphology, the general trend of the biofilm response was characterised by a decrease in biofilm biomass, thickness and surface area coupled with an important gain in roughness. The response was found dose dependent with impacts reported from 0.01 mg L^{-1}; therefore corroborating the sloughing phenomena reported *post* exposure to 0.02 - 2 mg L^{-1} Ag NPs elsewhere (Fabrega *et al*., 2009). In addition here, the microbial activity (*i.e*. monitored *via* the sole carbon source utilisation) was concomitantly shown to be time dependent (*i.e*. older and larger biofilms using more D-glucose in absence of NPs) as well as NP dose dependent (*i.e*. the utilisation of D-glucose being reduced *post* exposure to 10 mg L^{-1} Ag NPs and above). Consequently, the dose dependent biofilm restructuring previously mentioned did not involve an evident loss in the biofilm activity with the lowest concentrations of NPs (*i.e*. 0.01 - 1 mg L^{-1} range); instead the loss of activity was rather concomitant with the microbial death.

4.2. Potential mode of action for displayed Ag NP toxicity

Ag cations were reported to complex with the negatively charged extracellular matrix of the biofilms, potentially diminishing their bioavailability for an eventual toxicity (Habimana *et al*., 2011). However, Ag ions exhibited evident dose dependent toxic effects using non-static biofilms, as similarly discussed before with planktonic cultures (Losasso *et al*., 2014; Mallevre *et al*., 2014; Notter *et al*. 2014) and static biofilms (Choi *et al*., 2010; Radzig *et al*., 2013). The occurrence of the live/dead dual staining was also visibly increased in the assays in the case of the Ag ions, attesting to a superior biofilm-cidal pressure overall as previously stressed by Bjarnsholt *et al*. (2007) with Ag sulfadiazine. Similar observations were also reported with Zn^{2+} released ions from Zn NPs elsewhere (Hou *et al*., 2014); the tested Ag NPs were not therefore a single case example. The function, structure and extracellular matrix of *P. putida* biofilms were previously discussed as impacted by the surrounding nutrients (Bester *et al*., 2011; Jahn *et al*., 1999). The limited barrier role of the produced *P. putida* matrix due to the minimal conditions of growth in AW may therefore be

413 hypothesised here. The tested Ag NPs were nevertheless characterised by a low (*ca*. < 5 % in
414 mass) dissolution rate elsewhere (Klein *et al*., 2011; Mallevre *et al*., 2014); the observed
415 impacts of NPs cannot be supported solely by the released ions thus.

416 Interest has been recently shown in investigating the NP deposition onto and penetration
417 into biofilms. Peulen and Wilkinson (2011) reported that the relative self-diffusion
418 coefficients of several NPs (including Ag NPs) were decreased exponentially with the square
419 of the NP radius when tested with *Pseudomonas* spp. static biofilms. Choi *et al*. (2010)
420 showed that Ag NPs were able to penetrate *ca*. 40 µm in static biofilms within 1 h. From a
421 non-static biofilm viewpoint, Miller *et al*. (2013) showed that distributions of NPs through
422 the biofilms were consistent with diffusive transport and that uniform distributions through
423 the thickness were achieved within a few hours. Interactions between NPs and biofilms
424 were observed herein (*i.e*. impact on UV-vis spectra, loss in concentration as well as gain in
425 size and negative charges in effluent samples) and discussed previously (Fabrega *et al*.,
426 2009). NP deposition onto and penetration into the biofilms may therefore be proposed
427 here.

428 Consequently, the observed toxicity of tested Ag NPs (*ca*. 15 nm) is likely to be supported by
429 combined NP and ion based effects. Interestingly, the dose dependant and sequential
430 impact reported on biofilm morphology, viability and activity would support the hypothesis
431 of a NP dose dependent bacteriostatic (biofilm-static) and bactericidal (biofilm-cidal) like
432 response from non-static biofilms as previously suggested with static biofilms (Choi *et al*.,
433 2010; Dror Ehre *et al*., 2010; Inbakandan *et al*., 2013; Martinez-Gutierrez *et al*., 2013; Radzig
434 *et al*., 2013; Raftery *et al*., 2014). This would corroborate as well the notion of biofilm
435 adaptive stress response already described with other toxicants such as disinfectants
436 (Bridier *et al*., 2011).

437 ### 4.3. Long term effects

438 The importance of information regarding the long term effects of NPs was recently
439 emphasised (Fabrega *et al*., 2009; Handy *et al*., 2012). Nevertheless, such results using
440 biofilms are still to be reported in nano(eco)toxicology.

Herein, results from *P. putida* biofilms assessed 24 h *post* exposure to a single pulse of Ag NPs/ions showed overall recovering patterns on biofilm morphology and activity. In the absence of toxic pressure (*i.e*. the absence of NPs within the system during the recovery period was confirmed by AAS), biofilms were shown to restructure (*i.e*. presence of filaments and re-growth of microcolonies).

The formation of filaments by *P. putida* has been previously reported as an adaptive survival strategy in response to hostile conditions of growth (Crabbe *et al*., 2012; Jensen and Woolfolk, 1985). In fact, filament formation is a typical stress response to sub-lethal conditions displayed by a wide number of bacteria genera including *Escherichia coli*, *Listeria monocytogenes* and *Bacillus cereus* (Jones *et al*., 2013). It has been specifically reported in cases of pH, pressure and temperature stresses, of low water activity or high CO_2 conditions, and of antimicrobials presence (*e.g*. antibacterial peptides and disinfectants), however, we believe this is the first report of biofilm related filament formation in response to Ag NP stress conditions. Mechanisms of filament formation are commonly attributed to blockages in the early steps of the bacterial cell division due to a reduced energy state of the cell, mechanisms which were shown to be reversible (Jones *et al*., 2013). The formation of elongated bacteria was equally reported as a typical consequence of DNA damage and envelope stress (Justice *et al*., 2008). Interestingly, filaments were apparent only at 0.01 and 0.1 mg L^{-1} Ag NPs here, supporting the theory that filament formation is a dose dependent and reversible response as has been shown with other antimicrobial agents. We may in addition postulate that other filament producing bacteria (*e.g*. *Escherichia coli*, *Listeria monocytogenes* and *Bacillus cereus*) may similarly respond to Ag NPs under the same conditions.

Finally, variable results and potentially late effects were observed at 96 h *post* exposure to 1 mg L^{-1}. Accordingly to the NP mode of action afore hypothesised, some intermediate or threshold concentrations of NPs may then constitute a particularly “grey area” where mono-species biofilms display heterogeneous structure due to differing responses expressed at the single cell level.

4.4. Environmental relevance

The environmental concentration of NPs has been appraised around the µg L^{-1} range in surface waters and effluent wastewaters (Gottschalk *et al*., 2013). Despite morphological impacts being found from 0.01 mg L^{-1}, we demonstrated overall that biofilms exposed to pristine Ag NPs (up to 100 mg L^{-1}) were capable of morphological recovery within only 24 h. The microbial activity was not found significantly affected below 1 mg L^{-1} and was also subjected to recovery otherwise. In addition, Ag was shown sulphidised and interacting with organic matters in natural waters (Kaegi *et al*., 2013; Levard *et al*., 2012). We have shown that Ag NPs were less toxic and more subject to aggregation, especially with ageing, in real wastewaters than in artificial wastewaters (unpublished data). In light of this, the eventual impacts of released and aged Ag NPs in the µg L^{-1} range to *P. putida* biofilms may be therefore limited at the present time. Additional studies using other models would be necessary to extend the trends herein reported to natural biofilms.

The biofilm activity assessment was piloted herein using a D-glucose based monitoring. As the sole carbon source of the system, D-glucose utilisation appeared as a critical marker of the biofilm behaviour. Considering there is 1.07 mg of Chemical Oxygen Demand (COD) *per* mg of D-glucose, the theoretical COD removal activity may be estimated too. Being quicker, less sample consuming and easier to perform than the COD quantification; the D-glucose monitoring was preferred across conditions and experiments. Based on the original loading of D-glucose (0.5 %, w/v), ecotoxicity assays were performed in AW with an equivalent COD loading of *ca*. 5000 mg L^{-1}, corresponding to a high concentration case scenario. The use of D-glucose (in the 0.5 % range, w/v) was reported before (Bjarnsholt *et al*., 2007; Fabrega *et al*., 2009; Halan *et al*., 2011) in a similar AB trace minimal medium, minimal Davis medium or M9 medium. Fabrega *et al*. (2009) also worked, in addition, in the absence/presence (up to 10 mg L^{-1}) of humic substances. However, the correlation to C source utilisation or COD information was not considered in any of these studies. Additional assays related to the microbial activity (*e.g*. phosphorus or ammonium removal) may be anticipated for future works.

Although well described and still improving (Crusz *et al*., 2012; Weiss Nielsen *et al*., 2011; this work), macrofluidics systems as used here may still appear difficult to assemble and perform. A plethora of short term or long term as well as single and multiple pulse based

scenario with various NPs along with ageing and recovery assessment could be nonetheless piloted in order to help better mimic possible natural events and therefore better understand the real risk of NPs. At the present time though, there are scarce applications in nano(eco)toxicology with non-static mono-species biofilms (Fabrega *et al*., 2009; this work) and simply none with multi-species. Mix communities based non-static biofilms studies are consequently anticipated as future critical works in nano(eco)toxicology.

5. Conclusions

This paper reports for the first time on the temporal assessment of Ag NP and ion impact to the dynamics of mature *P. putida* based mono-species biofilms in parallelised flow-cells considering biofilm morphology, viability and activity related information.

Short term studies showed sequential dose dependent toxic effects of Ag NPs on *P. putida* biofilm morphology (with impacts characterised from 0.01 mg L^{-1}), then activity (from 1 - 10 mg L^{-1} range) and viability (from 10 mg L^{-1}) *via* a single pulse of 24 h in AW. Long term effects showed sequential dose dependant recovery of biofilm morphology and activity. Ag ions showed dose dependent impacts too but led to more efficient recovery *post* exposure despite being at least ten times more toxic than the tested Ag NPs. In lights of this and of the NP characterisation information, the combined effect of NPs and ions was proposed to support the observed toxicity results of tested Ag NPs.

Additional works using non-static biofilms are desirable in nano(eco)toxicology. Further studies on multi-species biofilms along with metabolomics, communities and extracellular matrix based temporal investigations are encouraged.

Acknowledgements

We would like to thank Heriot-Watt University (Edinburgh, UK) for providing FM with a James-Watt scholarship (Heriot-Watt University, Edinburgh, UK). We thank Dr C. Sternberg and Dr A. Heydorn (DTU, Lyngby, Denmark) for providing advice along with the COMSTAT 1 program. We acknowledge as well the European Union's Seventh Framework Programme [FP7 2007-2013] under EC-GA No. 263215 'MARINA', for the provision of the Ag NPs used in this study.

References

Bester, E., Kroukamp, O., Hausner, M., Edwards, E.A., Wolfaardt, G.M., 2011. Biofilm form and function: carbon availability affects biofilm architecture, metabolic activity and planktonic cell yield. *Journal of Applied Microbiology* 110, 387-398. DOI: 10.1111/j.1365-2672.2010.04894.x.

Bjarnsholt, T., Kirketerp-Moller, K., Kristiansen, S., Phipps, R., Nielsen, A.K., Jensen, P.O., Hoiby, N., Givskov, M., 2007. Silver against *Pseudomonas aeruginosa* biofilms. *APMIS* 115, 921-928. DOI: 10.1111/j.1600-0463.2007.apm_646.x.

Booth, S.C., Workentine, M.L., Wen, J., Shaykhutdinov, R., Vogel, H.J., Ceri, H., Turner, R.J., Weljie, A.M., 2011. Differences in metabolism between the biofilm and planktonic response to metal stress. *Journal of Proteome Research* 10, 3190-3199. DOI: 10.1021/pr2002353.

Bridier, A., Briandet, R., Thomas, V., Dubois-Brissonnet, F., 2011. Resistance of bacterial biofilms to disinfectants: a review. *Biofouling* 27, 1017-1032. DOI: 10.1080/08927014.2011.626899.

Buckingham-Meyer, K., Goeres, D.M., Hamilton, M.A., 2007. Comparative evaluation of biofilm disinfectant efficacy tests. *Journal of Microbiological Methods* 70, 236-244. DOI: 10.1016/j.mimet.2007.04.010.

Chernousova, S., Epple, M., 2013. Silver as antibacterial agent: ion, nanoparticle, and metal. *Angewandte Chemie International Edition* 52, 1636-1653. DOI: 10.1002/anie.201205923.

Choi, O.Y., Yu, C.P., Fernandez, G.E., Hu, Z.Q., 2010. Interactions of nanosilver with *Escherichia coli* cells in planktonic and biofilm cultures. *Water Research* 44, 6095-6103. DOI: 10.1016/j.watres.2010.06.069.

Crabbe, A., Leroy, B., Wattiez, R., Aertsen, A., Leys, N., Cornelis, P., Van Houdt, R., 2012. Differential proteomics and physiology of *Pseudomonas putida* KT2440 under filament-inducing conditions. *BMC Microbiology* 12. DOI: 10.1186/1471-2180-12-282.

553 Crusz, S.A., Popat, R., Rybtke, M.T., Camara, M., Givskov, M., Tolker-Nielsen, T., Diggle, S.P.,
554 Williams, P., 2012. Bursting the bubble on bacterial biofilms: a flow cell methodology.
555 *Biofouling* 28, 835-842. DOI: 10.1080/08927014.2012.716044.

556 Dong, X., Yang, L., 2014. Inhibitory effects of single-walled carbon nanotubes on biofilm
557 formation from *Bacillus anthracis* spores. *Biofouling* 30, 1165-1174. DOI:
558 10.1080/08927014.2014.975797.

559 Dror-Ehre, A., Adin, A., Markovich, G., Mamane, H., 2010. Control of biofilm formation in
560 water using molecularly capped silver nanoparticles. *Water Research* 44, 2601-2609. DOI:
561 10.1016/j.watres.2010.01.016.

562 Duester, L., Burkhardt, M., Gutleb, A.C., Kaegi, R., Macken, A., Meermann, B., von der
563 Kammer, F., 2014. Toward a comprehensive and realistic risk evaluation of engineered
564 nanomaterials in the urban water system. *Frontiers in chemistry* 2, 39. DOI:
565 10.3389/fchem.2014.00039.

566 Eduok, S., Martin, B., Villa, R., Nocker, A., Jefferson, B., Coulon, F., 2013. Evaluation of
567 engineered nanoparticle toxic effect on wastewater microorganisms: Current status and
568 challenges. *Ecotoxicology and Environmental Safety* 95, 1-9. DOI:
569 10.1016/j.ecoenv.2013.05.022.

570 Fabrega, J., Renshaw, J.C., Lead, J.R., 2009. Interactions of silver nanoparticles with
571 *Pseudomonas putida* biofilms. *Environmental Science & Technology* 43, 9004-9009. DOI:
572 10.1021/es901706j.

573 Fournier, E., 2001. Colorimetric quantification of carbohydrates, in: Wrolstad, R.E., Acree,
574 T.E., Decker, E.A., Penner, M.H., Reid, D.S., Schwartz, S.J., Shoemaker, C.F, Smith, D.M.,
575 Sporns, P. (Eds.), Current Protocols in Food Analytical Chemistry. John Wiley and Sons Inc.,
576 Unit E1.1. DOI: 10.1002/0471142913.fae0101s00.

577 Gottschalk, F., Sun, T.Y., Nowack, B., 2013. Environmental concentrations of engineered
578 nanomaterials: Review of modeling and analytical studies. *Environmental Pollution* 181, 287-
579 300. DOI: 10.1016/j.envpol.2013.06.003.

580 Habimana, O., Steenkeste, K., Fontaine-Aupart, M.-P., Bellon-Fontaine, M.-N., Kulakauskas,
581 S., Briandet, R., 2011. Diffusion of nanoparticles in biofilms is altered by bacterial cell wall
582 hydrophobicity. *Applied and Environmental Microbiology* 77, 367-368. DOI:
583 10.1128/AEM.02163-10.

584 Halan, B., Schmid, A., Buehler, K., 2011. Real-time solvent tolerance analysis of
585 *Pseudomonas* sp. strain LB120ΔC catalytic biofilms. *Applied and Environmental Microbiology*
586 77, 1563-1571. DOI: 10.1128/AEM.02498-10.

587 Hall-Stoodley, L., Costerton, J.W., Stoodley, P., 2004. Bacterial biofilms: From the natural
588 environment to infectious diseases. *Nature Reviews Microbiology* 2, 95-108. DOI:
589 10.1038/nrmicro821.

590 Handy, R.D., van den Brink, N., Chappell, M., Muehling, M., Behra, R., Dusinska, M.,
591 Simpson, P., Ahtiainen, J., Jha, A.N., Seiter, J., Bednar, A., Kennedy, A., Fernandes, T.F.,
592 Riediker, M., 2012. Practical considerations for conducting ecotoxicity test methods with
593 manufactured nanomaterials: what have we learnt so far? *Ecotoxicology* 21, 933-972. DOI:
594 10.1007/s10646-012-0862-y.

595 Heydorn, A., Nielsen, A.T., Hentzer, M., Sternberg, C., Givskov, M., Ersboll, B.K., Molin, S.,
596 2000. Quantification of biofilm structures by the novel computer program COMSTAT.
597 *Microbiology* 146, 2395-2407. DOI: 10.1099/00221287-146-10-2395.

598 Holden, P.A., Schimel, J.P., Godwin, H.A., 2014. Five reasons to use bacteria when assessing
599 manufactured nanomaterial environmental hazards and fates. *Current Opinion in*
600 *Biotechnology* 27, 73-78. DOI: 10.1016/j.copbio.2013.11.008.

601 Hou, J., Miao, L., Wang, C., Wang, P., Ao, Y., Qian, J., Dai, S., 2014. Inhibitory effects of ZnO
602 nanoparticles on aerobic wastewater biofilms from oxygen concentration profiles
603 determined by microelectrodes. *Journal of Hazardous Materials* 276, 164-170. DOI:
604 10.1016/j.jhazmat.2014.04.048.

605 Inbakandan, D., Kumar, C., Abraham, L.S., Kirubagaran, R., Venkatesan, R., Khan, S.A., 2013.
606 Silver nanoparticles with anti microfouling effect: A study against marine biofilm forming

607 bacteria. *Colloids and Surfaces B-Biointerfaces* 111, 636-643. DOI:
608 10.1016/j.colsurfb.2013.06.048.

609 Jahn, A., Griebe, T., Nielsen, P.H., 1999. Composition of *Pseudomonas putida* biofilms:
610 Accumulation of protein in the biofilm matrix. *Biofouling* 14, 49-57. DOI:
611 10.1080/08927019909378396.

612 Jensen, R.H., Woolfolk, C.A., 1985. Formation of filaments by *Pseudomonas putida*. *Applied*
613 *and Environmental Microbiology* 50, 364-372. DOI: 0099-2240/85/080364-09$02.00/0.

614 Jones, T.H., Vail, K.M., McMullen, L.M., 2013. Filament formation by foodborne bacteria
615 under sublethal stress. *International Journal of Food Microbiology* 165, 2, 97-110. DOI:
616 10.1016/j.ijfoodmicro.2013.05.001.

617 Ju-Nam, Y., Lead, J.R., 2008. Manufactured nanoparticles: An overview of their chemistry,
618 interactions and potential environmental implications. *Science of the Total Environment*
619 400, 396-414. DOI: 10.1016/j.scitotenv.2008.06.042.

620 Justice, S.S., Hunstad, D.A., Cegelski, L., Hultgren, S.J., 2008. Morphological plasticity as a
621 bacterial survival strategy. *Nature Reviews Microbiology* 6, 162-168. DOI:
622 10.1038/nrmicro1820.

623 Kaegi, R., Voegelin, A., Ort, C., Sinnet, B., Thalmann, B., Krismer, J., Hagendorfer, H.,
624 Elumelu, M., Mueller, E., 2013. Fate and transformation of silver nanoparticles in urban
625 wastewater systems. *Water Research* 47, 3866-3877. DOI: 10.1016/j.watres.2012.11.060.

626 Kahru, A., Ivask, A., 2013. Mapping the dawn of nanoecotoxicological research. *Accounts of*
627 *Chemical Research* 46, 823-833. DOI: 10.1021/ar3000212.

628 Klein, C., Comero, S., Stahlmecke, B., Romazanov, J., Kuhlbusch, T., van Doren, E., Wick, P.,
629 Locoro, G., Koerdel, W., Gawlik, B., Mast, J., Krug, H. F., Hund-Rinke, K., Friedrichs, S., Maier,
630 G., Werner, J., Linsinger, T., 2011. NM-300 silver characterisation, stability, homogeneity.
631 EUR – Scientific and Toxicological Sciences, Technical Research Reports, JRC Publication No.
632 JRC60709, EUR 24693 EN, Publications Office of the European Union. DOI: 10.2788/23079.

633 Levard, C., Hotze, E.M., Lowry, G.V., Brown, G.E., 2012. Environmental transformations of
634 silver nanoparticles: Impact on stability and toxicity. *Environmental Science & Technology*
635 46, 6900-6914. DOI: 10.1021/es2037405.

636 Losasso, C., Belluco, S., Cibin, V., Zavagnin, P., Micetic, I., Gallocchio, F., Zanella, M., Bregoli,
637 L., Biancotto, G., Ricci, A., 2014. Antibacterial activity of silver nanoparticles: Sensitivity of
638 different *Salmonella* serovars. *Frontiers in Microbiology* 5. DOI: 10.3389/fmicb.2014.00227.

639 Mallevre, F., Fernandes, T.F., Aspray, T.J., 2014. Silver, zinc oxide and titanium dioxide
640 nanoparticle ecotoxicity to bioluminescent *Pseudomonas putida* in laboratory medium and
641 artificial wastewater. *Environmental Pollution* 195, 218-225. DOI:
642 10.1016/j.envpol.2014.09.002.

643 Martinez-Gutierrez, F., Boegli, L., Agostinho, A., Sanchez, E.M., Bach, H., Ruiz, F., James, G.,
644 2013. Anti-biofilm activity of silver nanoparticles against different microorganisms.
645 *Biofouling* 29, 651-660. DOI: 10.1080/08927014.2013.794225.

646 Miller, J.K., Neubig, R., Clemons, C.B., Kreider, K.L., Wilber, J.P., Young, G.W., Ditto, A.J., Yun,
647 Y.H., Milsted, A., Badawy, H.T., Panzner, M.J., Youngs, W.J., Cannon, C.L., 2013. Nanoparticle
648 deposition onto biofilms. *Annals of Biomedical Engineering* 41, 53-67. DOI: 10.1007/s10439-
649 012-0626-0.

650 Morones, J.R., Elechiguerra, J.L., Camacho, A., Holt, K., Kouri, J.B., Ramirez, J.T., Yacaman,
651 M.J., 2005. The bactericidal effect of silver nanoparticles. *Nanotechnology* 16, 2346-2353.
652 DOI: 10.1088/0957-4484/16/10/059.

653 Notter, D.A., Mitrano, D.M., Nowack, B., 2014. Are nanosized or dissolved metals more toxic
654 in the environment? A meta-analysis. *Environmental Toxicology and Chemistry* 33, 2733-
655 2739. DOI: 10.1002/etc.2732.

656 Park, H.J., Park, S., Roh, J., Kim, S., Choi, K., Yi, J., Kim, Y., Yoon, J., 2013. Biofilm-inactivating
657 activity of silver nanoparticles: A comparison with silver ions. *Journal of Industrial and*
658 *Engineering Chemistry* 19, 614-619. DOI: 10.1016/j.jiec.2012.09.013.

Peulen, T.O., Wilkinson, K.J., 2011. Diffusion of nanoparticles in a biofilm. *Environmental Science & Technology* 45, 3367-3373. DOI: 10.1021/es103450g.

Radzig, M.A., Nadtochenko, V.A., Koksharova, O.A., Kiwi, J., Lipasova, V.A., Khmel, I.A., 2013. Antibacterial effects of silver nanoparticles on gram-negative bacteria: Influence on the growth and biofilms formation, mechanisms of action. *Colloids and Surfaces B-Biointerfaces* 102, 300-306. DOI: 10.1016/j.colsurfb.2012.07.039.

Raftery, T.D., Kerscher, P., Hart, A.E., Saville, S.L., Qi, B., Kitchens, C.L., Mefford, O.T., McNealy, T.L., 2014. Discrete nanoparticles induce loss of *Legionella pneumophila* biofilms from surfaces. *Nanotoxicology* 8, 477-484. DOI: 10.3109/17435390.2013.796537.

Rai, M., Birla, S., Ingle, A.P., Gupta, I., Gade, A., Abd-Elsalam, K., Marcato, P.D., Duran, N., 2014. Nanosilver: an inorganic nanoparticle with myriad potential applications. *Nanotechnology Reviews* 3, 281-309. DOI: 10.1515/ntrev-2014-0001.

Skogman, M.E., Vuorela, P.M., Fallarero, A., 2012. Combining biofilm matrix measurements with biomass and viability assays in susceptibility assessments of antimicrobials against *Staphylococcus aureus* biofilms. *Journal of Antibiotics* 65, 453-459. DOI: 10.1038/ja.2012.49.

Stewart, P.S., Franklin, M.J., 2008. Physiological heterogeneity in biofilms. *Nature Reviews Microbiology* 6, 199-210. DOI: 10.1038/nrmicro1838.

Tote, K., Horemans, T., Vanden Berghe, D., Maes, L., Cos, P., 2010. Inhibitory effect of biocides on the viable masses and matrices of *Staphylococcus aureus* and *Pseudomonas aeruginosa* biofilms. *Applied and Environmental Microbiology* 76, 3135-3142. DOI: 10.1128/AEM.02095-09.

Weiss Nielsen, M., Sternberg, C., Molin, S., Regenberg, B., 2011. *Pseudomonas aeruginosa* and *Saccharomyces cerevisiae* biofilm in flow cells. *Journal of visualized experiments: JOVE.* DOI: 10.3791/2383.

Wiles, S., Whiteley, A.S., Philp, J.C., Bailey, M.J., 2003. Development of bespoke bioluminescent reporters with the potential for in situ deployment within a phenolic-

remediating wastewater treatment system. *Journal of Microbiological Methods* 55, 667-677. DOI: 10.1016/S0167-7012(03)00203-3.

687 **Supplementary material**

688

689

690

691

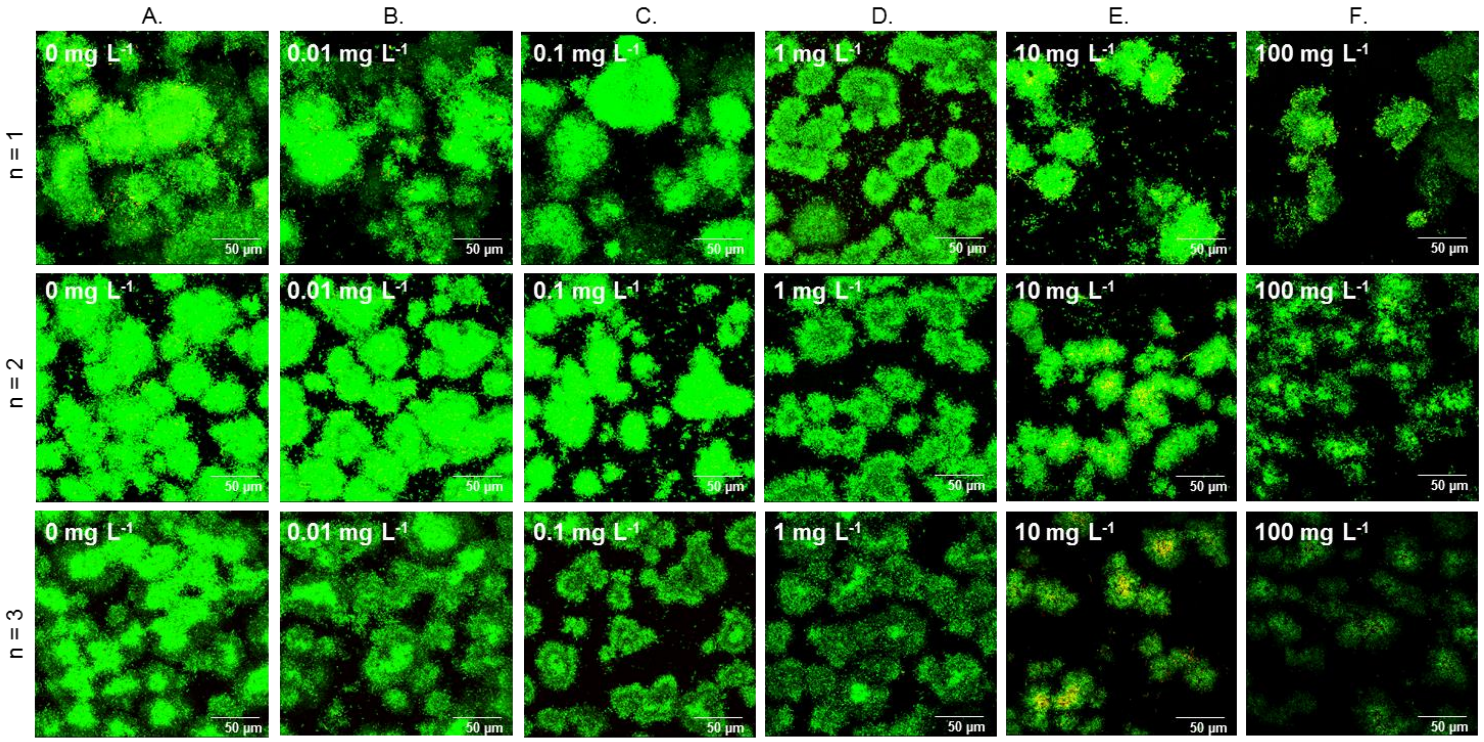

692

693 **Fig. S1: Biofilm morphology characterisation *post* exposure to Ag NM-300K NPs.** Additional
694 examples of result at 72 h (*i.e*. *post* exposure) from three replicate experiments are presented above
695 as support for the Figure 2 (bottom row), therefore the same caption applies.

696

697

698

699

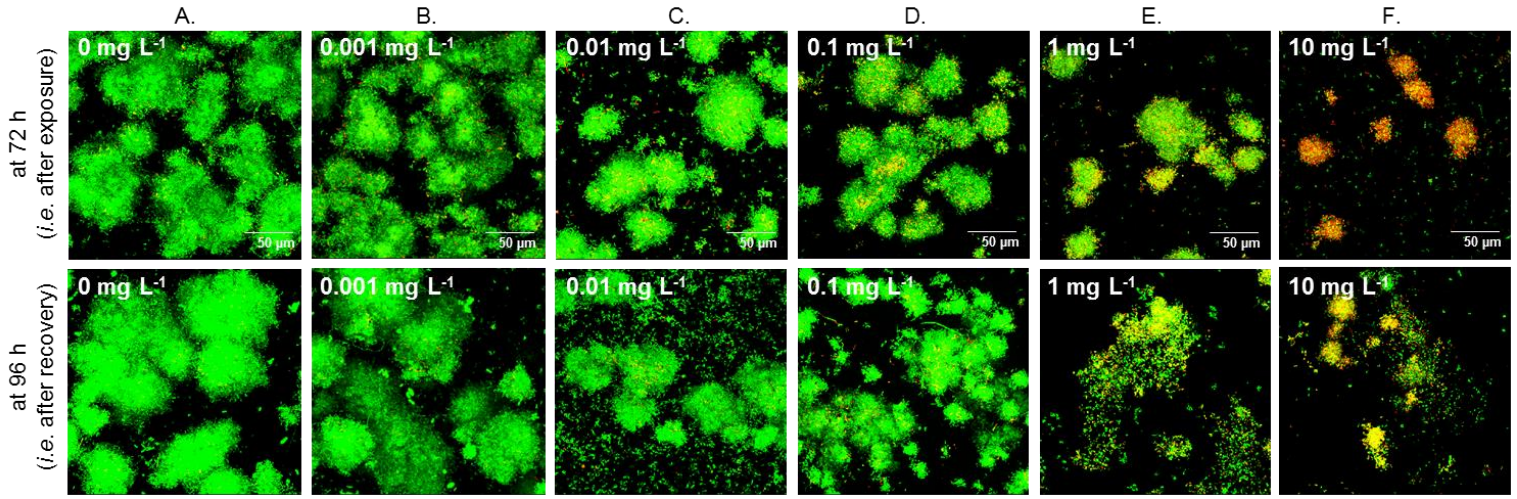

Fig. S2: Biofilm morphology characterisation *post* exposure to Ag ions. *Pseudomonas putida* mono-species biofilms were cultured in artificial wastewater in CLSM compatible flow-cells for 48 h then exposed to 0, 0.001, 0.01, 0.1, 1 and 10 mg L^{-1} of Ag ions for 24 h (from A to F respectively). Biofilms were analysed by CLSM after live/dead staining at 72 h (*i.e. ante* exposure, top row) and at 96 h (*i.e. post* recovery, bottom row). Representative examples of maximised z-stack are shown. Each image represents 1 out of 7 z-stacks randomly registered *per* condition for 1 experiment (n = 3). Scale is 50 µm wide.

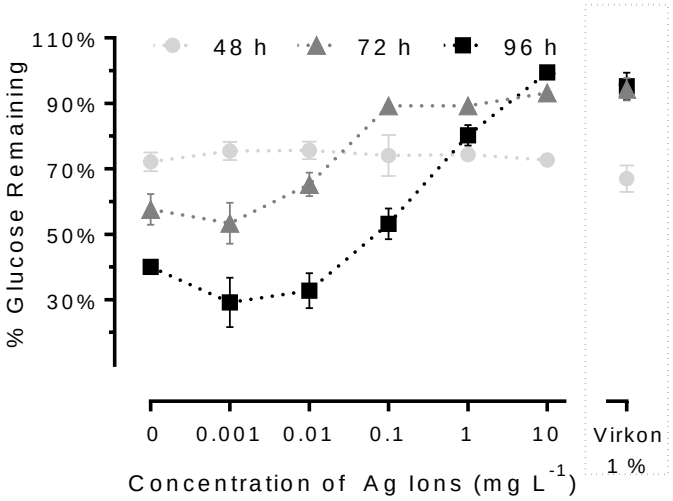

Fig. S3: Quantitative characterisation of the microbial activity (Ag ion case). Samples collected upstream (*i.e*. in influents) and downstream (*i.e*. in effluents) of the flow-cells at 48, 72 and 96 h were used for D-glucose quantification *via* the phenol - sulphuric acid assay. Presented data are mean ± SEM (n = 3) of the calculated percentages of D-glucose remaining (in % terms) in effluents *per* tested condition. The detailed findings from the statistical analysis *via* multiple t-tests (corrected with the Holm-Sidak method) considering two parameters at a time are shown in Figure S4.

	48 h vs 72 h	72 h vs 96 h	48 h vs 96 h
0 mg L^{-1}	**⇗	**⇗	**⇗
0.01 (0.001) mg L^{-1}	**⇗ (**⇗)	NSD (*⇗)	**⇗ (**⇗)
0.1 (0.01) mg L^{-1}	*⇗ (*⇗)	NSD (**⇗)	**⇗ (**⇗)
1 (0.1) mg L^{-1}	*⇗ (*⇘)	NSD (**⇗)	**⇗ (*⇗)
10 (1) mg L^{-1}	NSD (**⇘)	NSD (*⇗)	NSD (NSD)
100 (10) mg L^{-1}	**⇘ (**⇘)	NSD (NSD)	NSD (**⇘)
Virkon 1 %	**⇘	NSD	**⇘

Fig. S4: Statistical analysis of the reported microbial activity results. The output results from the statistical analysis *via* multiple t-tests (corrected with the Holm-Sidak method) considering two parameters at a time are shown. The NP case is reported in blue, the ion case in red. Significantly different between time points (increased or decreased activity over time) with a *p value* < 0.1 (*) or < 0.05 (**). Non-significantly different (NSD).

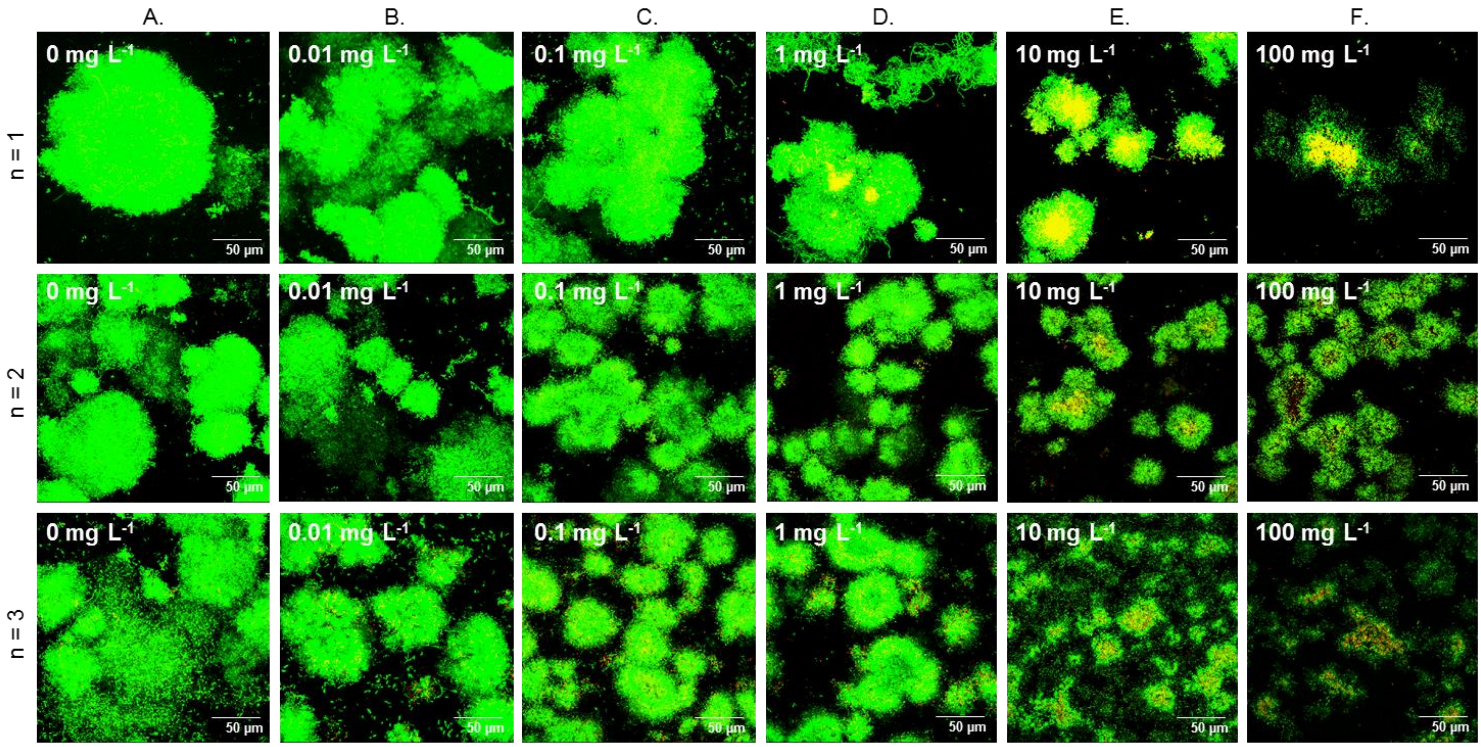

Fig. S5: Biofilm recovery assessment *post* exposure to Ag NM-300K NPs. Supplementary examples of result at 96 h (*i.e. post* recovery) from three replicate experiments are presented above as support for the Figure 5, therefore the same caption applies.